Available online at www.sciencedirect.com

ScienceDirect

Physics Letters A

Physics Letters A 00 (2025) 1–7

Double attenuation peaks in metamaterial with simultaneous negative mass and stiffness

Abhigna Bhatt[a], Arnab Banerjee[a]

[a]*Department of Civil Engineering, Indian Institute of Technology Delhi, India*

Abstract

Wider bandgap and band merging phenomena in simultaneous negative mass and stiffness metamaterial were reported and studied previously. In this letter, an additional feature, namely double attenuation peak, of simultaneous negative mass and stiffness metamaterial has been identified. The generation of double attenuation peaks is hinged upon the resonance coupling of longitudinal and transverse resonator. Double attenuation peaks ensures a significant level of spatial attenuation throughout the attenuation band.

© 2021 Published by Elsevier Ltd.

Keywords: Bloch theorem, negative mass, negative stiffness, double peak

1. Introduction

The metamaterial has unique property of observing frequency dependant dynamic mass and stiffness, owing to this a sub-wavelength attenuation bandgap is resulted. This frequency dependent mass and stiffness are generally termed as effective mass (M_{eff}) and effective stiffness (K_{eff}) [1–3]. Researchers has proposed several systems to obtain negative Young's modulus or stiffness [4–10] as well as negative mass in metamaterial [11–13]. In the field of acoustic and elastic metamaterial, the simultaneous negative density and modulus is also widely investigated by several researchers [14–30] owing to its salient feature of generation of local resonance (LR) bandgaps. These LR bands enable to remove the size constrain of the structure [31] which essentially provides a flexibility in designing and realizing real system, such as Helmholtz resonator [32, 33]. The metamaterial with effective negative mass has been exemplified by plasma oscillations in metal particles [11, 34]. The group velocity, phase velocity, and merging of attenuation bands towards obtaining a wider attenuation bandgap were the primary focus of the simultaneous negative metamaterial [18, 35] in the existing state of the art. As all the above mentioned attributes can be obtained from the real part of the dispersion relationship; hence very little attention were given in the plotting of imaginary part of the dispersion

Email addresses: abhigna.bhatt@gmail.com (Abhigna Bhatt), abanerjee@iitd.ac.in (Arnab Banerjee)

relationship. In this paper, we have shedded light on the imaginary part of the dispersion relationship to comprehend the strength of the spatial attenuation of the waves within the attenuation band[36]. In order to cater the above mentioned objective, the simultaneous negative mass and stiffness metamaterial proposed by Huang and Sun [18] as shown in Fig. 1-(a) is adopted and the methodology is extended further to plot the imaginary part of the dispersion relationship. Additionally, the effective mass and effective stiffness are plotted in frequency domain to develop further insight about the attenuation strength.

2. Methodology

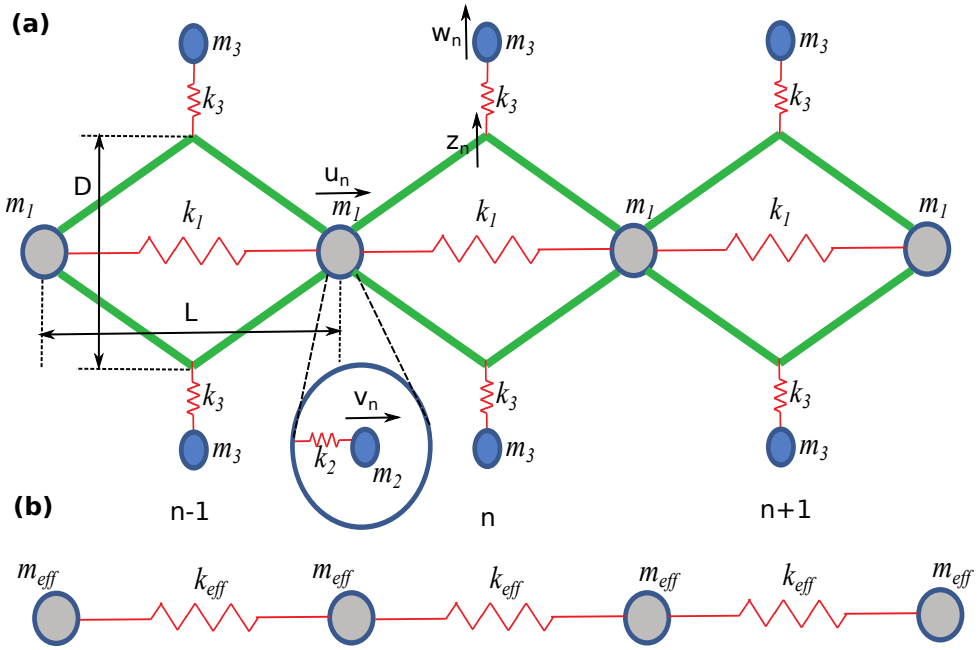

Fig. 1. (a) Model of simultaneous negative metamaterial (b) Monoatomic chain model

An acoustic metamaterial is modelled by assembling mass in mass unit with resonator attached to massless rigid link as shown in Fig. 1-(a) [18]. m_1 is outer ring mass; m_2 and k_2 is mass and stiffness of resonator placed in mass in mass unit. k_1 is stiffness connecting two mass in mass unit. m_3 and k_3 are mass and stiffness of resonator connected by massless rigid link as shown in Fig. 1-(a). u_n, v_n and w_n are only degrees of freedom of masses respectively m_1, m_2 and m_3 of n^{th} unit cell. z_n is the degree of freedom at connection of rigid links with spring k_3 of n^{th} unit cell. L is the distance between to outer ring masses m_1 and D is the distance between two rigid link connections with spring k_3 as shown in Fig. 1-(a). The governing equations for the acoustic metamaterial (Fig. 1-(a)) can be written as [18].

$$\begin{aligned} m_1\ddot{u}_n + k_1(2u_n - u_{n-1} - u_{n+1}) - k_2(v_n - u_n) - 2k_3(w_n - z_n) + 2k_3(w_{n-1} - z_{n-1}) &= 0 \\ m_2\ddot{v}_n + k_2(v_n - u_n) &= 0 \\ m_3\ddot{w}_n + k_3(w_n - z_n) &= 0 \end{aligned} \tag{1}$$

The displacement compatibility is obtained as [18].

$$z_n = -\frac{L}{2D}\left(u_{n+1} - u_n\right) \tag{2}$$

The displacement of n^{th} atom of metamaterial can be assumed as [19].

$$u_n(t) = \tilde{u}_n(\omega)\, e^{-i\,\omega\, t} \tag{3}$$

where,$\tilde{u}_n$ is frequency dependant amplitude of n^{th} unit and ω is temporal frequency. As per the Bloch theorem [37]

$$\tilde{u}_{n-1} = \tilde{u}_n\, e^{-iL\kappa} = \tilde{u}_n\, e^{-i\xi} \tag{4}$$

where, L is distance between two consecutive unit cells, κ is a wave number and ξ is a nondimentional wave number also called as propagation constant [38]. The effective mass of the system can be calculated using the conservation of mass momentum in longitudinal direction Eq. 5.

$$M_{eff}\,\dot{u}_n = m_1\,\dot{u}_n + m_2\,\dot{v}_n \tag{5}$$

The equation for the dispersion relation of the acoustic metametrial given in Fig. 1 can be obtained by deriving effective mass and stiffness and plugging them into the dispersion relation equation of a monoatomic chain (Fig. 1-(b)) [36]. Effective mass (M_{eff}) and effective stiffness (K_{eff}) as functions of frequency (ω) have been obtained as

$$M_{eff} = m_1 - \frac{m_2}{\frac{m_2\,\omega^2}{k_2} - 1} \tag{6}$$

$$K_{eff} = k_1 + \frac{\omega^2 L^2 m_3}{2D^2}\left(\frac{m_3\,\omega^2}{k_3} - 1\right)^{-1} \tag{7}$$

The dispersion relation is described by

$$\begin{aligned} -M_{eff}\,\omega^2 + K_{eff}\,\left(2 - 2\cos(\xi)\right) &= 0 \\ \xi = \cos^{-1}\left(1 - \frac{\omega^2\, M_{eff}}{2\, K_{eff}}\right) & \end{aligned} \tag{8}$$

From Eq. 8, it is expected that in case of $|\frac{\omega^2\, M_{eff}}{2\, K_{eff}}| > 1$, the propagation constant ξ will have a non zero imaginary value ($\xi = \alpha + \beta\, i$). The equation of forward wave propagation can be written as

$$\tilde{u}_{n+1} = \tilde{u}_n\, e^{i\xi} = \tilde{u}_n\, e^{i(\alpha+\beta\, i)} = \tilde{u}_n\, e^{-\beta}\left(\cos(\alpha) + i\,\sin(\alpha)\right) \tag{9}$$

$e^{-\beta}$ in Eq. 9 elucidates spatial exponential decay of the wave amplitude in the forward wave propagation. Further, the rate of attenuation in space increases with increase with β, so β is defined as the level or strength of attenuation. It can also be concluded that higher value of β is another coveted feature of the metamaterial. The conditions for peak in attenuation band can be defined as

$$\begin{aligned} K_{eff} = 0 \text{ or } M_{eff} \to \infty & \\ \Rightarrow \cos(\xi) \to \infty,\ \text{So } \beta \to \infty & \end{aligned} \tag{10}$$

Table 1. Non-dimensional Input parameters

Case	Mass ratio		Stiffness ratio		
	θ_{21}	θ_{31}	δ_{21}	δ_{31}	μ
1	1.5	1	0.1	1	1.67
2	2.25	0.4	0.3	0.25	5

Solving $K_{eff} = 0$

$$\omega_s = \sqrt{\frac{k_1\, k_3\, m_3}{k_1 + 0.5\,(L/D)^2\, m_3}} \tag{11}$$

Solving $M_{eff} = \infty$

$$\omega_m = \sqrt{k_2/m_2} \tag{12}$$

where, ω_s and ω_m are frequencies at which peak will occur respectively due to negative stiffness and negative mass in attenuation band. Now, the boundary of propagation band can be obtained by [39]

$$-1 \leq 1 - \frac{\omega^2\, M_{eff}}{2\, K_{eff}} \leq 1 \tag{13}$$

When both the frequencies ω_s and ω_m lies in between two consecutive boundaries obtained from Eq. 13, the double peak in single attenuation band will occur.

3. Results

In this paper, two cases are considered for the illustration and validation as shown in Fig. 2. In case-1 simultaneous negative mass and stiffness are not found; whereas, in case-2 it is observed [18]. The parameters has been nondimensionalised for calculation and validation as following.

$$\theta_{21} = \frac{m_2}{m_1};\;\; \theta_{31} = \frac{m_3}{m_1};\;\; \delta_{21} = \frac{k_2}{k_1};\;\; \delta_{31} = \frac{k_3}{k_1};\;\; \mu = \left(\frac{L}{D}\right)^2 \tag{14}$$

frequency ratio (η), peaks frequency ratio due to negative mass(η_m) and stiffness(η_s) are nondimensionalised as

$$\eta = \frac{\omega}{\sqrt{k_2/m_2}};\;\; \eta_m = \frac{\omega_m}{\sqrt{k_2/m_2}}\;\; \eta_s = \frac{\omega_s}{\sqrt{k_2/m_2}} \tag{15}$$

The input parameters for both cases are given in Table 1. Further, propagation constant (ξ), effective mass (M_{eff}) and effective stiffness (K_{eff}) are plotted (Fig. 2) against frequency ratio (η) for validation with [18]. Fig. 2(b) and (e) validates that the real part of dispersion curve for both the cases are in complete agreement with results reported in [18]. The bounds (b_1, b_2, b_3, b_4 and b_5) and peak frequency ratios for infinite M_{eff} and zero K_{eff} calculated respectively from Eq. 11,Eq. 12 and Eq. 13 are tabulated in Table 2. It can be comprehended from Table 2 and Fig. 2 that in case-1, both the attenuation peak lies in different bandgap

$$b_2 < \eta_m < b_3,\;\; b_4 < \eta_s < b_5$$

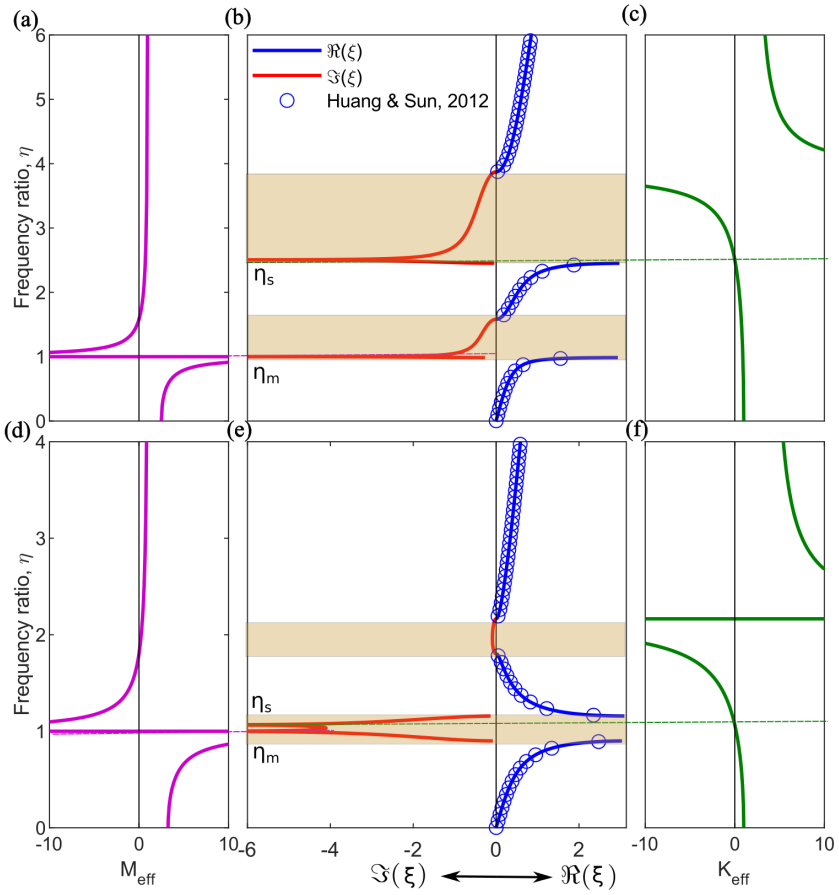

Fig. 2. (a) Effective mass of case-1, (b) Dispersion curves for case-1, (c) Effective stiffness of case-1,(d) Effective mass of case-2, (e) Dispersion curves for case-2, (f) Effective stiffness of case-2. Dashed purple line depicts the peak in attenuation band due to $M_{eff} \to \infty$ at η_m and Dashed green line depicts the peak in attenuation band due to $K_{eff} = 0$ at η_s

where as, in case-2, both the peaks lie in a same bandgap as the frequency of both the resonators are in closed proximity.

$$b_2 < \eta_m,\ \eta_s < b_3$$

This leads to coupling between the two resonators. Due to double peak in a single band, high level of attenuation ($\beta = 4$) is observed for major part of attenuation band unlike other attenuation bands. Therefore, a significant decay of wave amplitude is expected in spatial domain.

4. Conclusion

The attenuation characteristics, effective mass and effective stiffness of acoustic metamaterial with simultaneous negative mass and stiffness has been investigated and validated in this study. Further the rate of attenuation in spatial domain has been calculated by

Table 2. Output parameters

	Bounds of bandgap					Peak	
Case	b_1	b_2	b_3	b_4	b_5	η_m	η_s
1	0	0.986	1.581	2.449	12.417	1.000	2.506
2	0	0.900	1.158	1.803	11.381	1.000	1.068

considering imaginary part of the propagation constant. Coupling occurs while the natural frequencies of the two resonators are in close proximity. This results to a noteworthy double peak phenomenon in a single attenuation band which provides a significant spatial attenuation rate throughout the attenuation bandgap.

References

[1] G. Hong, J. Li, J. Pan, J. Fang, H. Li, Mass and stiffness identification of particle beam system based on a dynamic effective mass method, Journal of Vibration and Control 27 (15-16) (2021) 1920–1926.

[2] S. Adhikari, T. Mukhopadhyay, A. Shaw, N. Lavery, Apparent negative values of young's moduli of lattice materials under dynamic conditions, International Journal of Engineering Science 150 (2020) 103231.

[3] L. Shen, Z. Wang, X. Wang, K. Wei, Negative poisson's ratio and effective young's modulus of a vertex-based hierarchical re-entrant honeycomb structure, International Journal of Mechanical Sciences 206 (2021) 106611.

[4] Z.-X. Lu, X. Li, Z.-Y. Yang, F. Xie, Novel structure with negative poisson's ratio and enhanced young's modulus, Composite Structures 138 (2016) 243–252.

[5] F. Lin, Y. Xiang, H.-S. Shen, Tunable positive/negative young's modulus in graphene-based metamaterials, Advanced Theory and Simulations 4 (2) (2021) 2000130.

[6] T.-C. Lim, An auxetic metamaterial with tunable positive to negative hygrothermal expansion by means of counter-rotating crosses, physica status solidi (b).

[7] X.-L. Peng, S. Bargmann, A novel hybrid-honeycomb structure: Enhanced stiffness, tunable auxeticity and negative thermal expansion, International Journal of Mechanical Sciences 190 (2021) 106021.

[8] A. Dwivedi, A. Banerjee, B. Bhattacharya, Simultaneous energy harvesting and vibration attenuation in piezo-embedded negative stiffness metamaterial, Journal of Intelligent Material Systems and Structures 31 (8) (2020) 1076–1090.

[9] C. Ren, Q. Li, D. Yang, Quasi-static and sound insulation performance of a multifunctional cylindrical cellular shell with bidirectional negative-stiffness metamaterial cores, International Journal of Mechanical Sciences 180 (2020) 105662.

[10] X. Tan, S. Chen, B. Wang, J. Tang, L. Wang, S. Zhu, K. Yao, P. Xu, Real-time tunable negative stiffness mechanical metamaterial, Extreme Mechanics Letters 41 (2020) 100990.

[11] E. Bormashenko, I. Legchenkova, Negative effective mass in plasmonic systems, Materials 13 (8) (2020) 1890.

[12] Z. Yang, J. Mei, M. Yang, N. Chan, P. Sheng, Membrane-type acoustic metamaterial with negative dynamic mass, Physical review letters 101 (20) (2008) 204301.

[13] C. T. Chan, J. Li, K. H. Fung, On extending the concept of double negativity to acoustic waves, Journal of Zhejiang University-SCIENCE A 7 (1) (2006) 24–28.

[14] Y. Ding, Z. Liu, C. Qiu, J. Shi, Metamaterial with simultaneously negative bulk modulus and mass density, Physical review letters 99 (9) (2007) 093904.

[15] S. H. Lee, C. M. Park, Y. M. Seo, Z. G. Wang, C. K. Kim, Composite acoustic medium with simultaneously negative density and modulus, Physical review letters 104 (5) (2010) 054301.

[16] L. Fok, X. Zhang, Negative acoustic index metamaterial, Physical Review B 83 (21) (2011) 214304.

[17] X.-N. Liu, G.-K. Hu, G.-L. Huang, C.-T. Sun, An elastic metamaterial with simultaneously negative mass density and bulk modulus, Applied physics letters 98 (25) (2011) 251907.

[18] H.-H. Huang, C.-T. Sun, Anomalous wave propagation in a one-dimensional acoustic metamaterial having simultaneously negative mass density and young's modulus, The Journal of the Acoustical Society of America 132 (4) (2012) 2887–2895.
[19] A. Banerjee, R. Das, E. P. Calius, Waves in structured mediums or metamaterials: a review, Archives of Computational Methods in Engineering 26 (4) (2019) 1029–1058.
[20] T. Terao, Wave propagation in double-negative acoustic metamaterial multilayers, in: 2020 Fourteenth International Congress on Artificial Materials for Novel Wave Phenomena (Metamaterials), IEEE, pp. 418–420.
[21] S. Lin, Y. Zhang, Y. Liang, Y. Liu, C. Liu, Z. Yang, Bandgap characteristics and wave attenuation of metamaterials based on negative-stiffness dynamic vibration absorbers, Journal of Sound and Vibration 502 (2021) 116088.
[22] H. Chen, C. Ding, Simulated and experimental research of multi-band acoustic metamaterial with a single resonant structure, Materials 12 (21) (2019) 3469.
[23] A. Srivastava, Elastic metamaterials and dynamic homogenization: a review, International Journal of Smart and Nano Materials 6 (1) (2015) 41–60.
[24] C. Li, T. Jiang, Q. He, Z. Peng, Stiffness-mass-coding metamaterial with broadband tunability for low-frequency vibration isolation, Journal of Sound and Vibration 489 (2020) 115685.
[25] A. Sridhar, L. Liu, V. Kouznetsova, M. Geers, Homogenized enriched continuum analysis of acoustic metamaterials with negative stiffness and double negative effects, Journal of the Mechanics and Physics of Solids 119 (2018) 104–117.
[26] S. Sang, A. Mhannawee, Z. Wang, A design of active elastic metamaterials with negative mass density and tunable bulk modulus, Acta Mechanica 230 (3) (2019) 1003–1008.
[27] W. Wang, B. Bonello, B. Djafari-Rouhani, Y. Pennec, J. Zhao, Double-negative pillared elastic metamaterial, Physical Review Applied 10 (6) (2018) 064011.
[28] Z. Li, C. Wang, X. Wang, Modelling of elastic metamaterials with negative mass and modulus based on translational resonance, International Journal of Solids and Structures 162 (2019) 271–284.
[29] A. A. Mokhtari, Y. Lu, A. Srivastava, On the emergence of negative effective density and modulus in 2-phase phononic crystals, Journal of the Mechanics and Physics of Solids 126 (2019) 256–271.
[30] J. H. Oh, H. M. Seung, Y. Y. Kim, Doubly negative isotropic elastic metamaterial for sub-wavelength focusing: Design and realization, Journal of Sound and Vibration 410 (2017) 169–186.
[31] H. Al Ba'ba'a, M. Nouh, T. Singh, Formation of local resonance band gaps in finite acoustic metamaterials: A closed-form transfer function model, Journal of Sound and Vibration 410 (2017) 429–446.
[32] Y. Cheng, J. Xu, X. Liu, One-dimensional structured ultrasonic metamaterials with simultaneously negative dynamic density and modulus, Physical Review B 77 (4) (2008) 045134.
[33] C. Yilmaz, Identifying different phononic band gap generation methods, in: 5th International Conference on Phononic Crystals/Metamaterials, Phonon Transport and Topological Phononics, Tucson, Arizona, USA, 2019, pp. 23–24.
[34] E. Bormashenko, I. Legchenkova, M. Frenkel, Negative effective mass in plasmonic systems ii: elucidating the optical and acoustical branches of vibrations and the possibility of anti-resonance propagation, Materials 13 (16) (2020) 3512.
[35] O. Yuksel, C. Yilmaz, Realization of an ultrawide stop band in a 2-d elastic metamaterial with topologically optimized inertial amplification mechanisms, International Journal of Solids and Structures 203 (2020) 138–150.
[36] A. Banerjee, S. Adhikari, M. I. Hussein, Inertial amplification band-gap generation by coupling a levered mass with a locally resonant mass, International Journal of Mechanical Sciences 207 (2021) 106630.
[37] F. Bloch, Über die quantenmechanik der elektronen in kristallgittern, Zeitschrift für physik 52 (7) (1929) 555–600.
[38] A. Baxy, R. Prasad, A. Banerjee, Elastic waves in layered periodic curved beams, Journal of Sound and Vibration 512 (2021) 116387.
[39] D. J. Mead, Wave propagation and natural modes in periodic systems: I. mono-coupled systems, Journal of Sound and Vibration 40 (1) (1975) 1–18.